A Case Study of Surface Roughness Improvement for C40 Carbon Steel and 201 Stainless Steel using Ultrasonic Assisted Vibration in Cutting Speed Direction

Thanh Trung Nguyen
School of Mechanical Engineering, Hanoi University of Science and Technology, Vietnam
trung.nguyenthanh2@hust.edu.vn

Truong Cong Tuan
School of Mechanical Engineering, Hanoi University of Science and Technology, Vietnam
tuan.truongcong@hust.edu.vn

Toan Thang Vu
School of Mechanical Engineering, Hanoi University of Science and Technology, Vietnam
thang.vutoan@hust.edu.vn (corresponding author)

Received: 19 April 2024 2024 | Revised: 7 May 2024 | Accepted: 11 May 2024

 DOI: https://doi.org/10.48084/etasr.7552

ABSTRACT

The surface roughness of mechanical parts plays an important role in evaluating the machining performance. However, achieving fine surface finishes on small-diameter shafts through traditional lathes poses challenges due to low cutting speed and workpiece stiffness. To address this issue, in the present work, we applied ultrasonic-assisted vibration aligned with the cutting speed direction to enhance the turning process of small shafts made of C40 Carbon steel or 201 stainless steel. The workpieces were machined by Ultrasonic Assisted Turning (UAT) at three different cutting speeds, ranging from 15 to 36 m/min, while maintaining a constant feed rate and depth of cut. To facilitate comparison with conventional turning (CT), the cutting parameters remained consistent, and both methods were performed for the same duration. UAT necessitates the use of a specialized turning inserts' fixture known as a horn to transmit ultrasonic vibrations from the generator to the tooltip. This study also presents the design methodology and the performance evaluation of the horn. Surface roughness was assessed using the arithmetical mean height, Ra. In UAT, the roughness Ra exhibited the most significant reduction for C40 Carbon steel, reaching a decrease of 308% at a cutting speed of 15 m/min, whereas for 201 stainless steel, Ra did not vary by more than 23% across different cutting speeds.

Keywords-surface roughness; ultrasonic vibration; cutting speed direction; sampling frequency; laser displacement sensor

I. INTRODUCTION

Small pins serve diverse functions in various industries, encompassing pressure die casting, automotive and aerospace manufacturing. In pressure die casting, these pins play the role of ejecting the molded part from the mold cavity once the molding cycle is over. Likewise, in injection molding, core pins are utilized to create internal features or cavities within the molded part. By inserting these pins into the mold cavity, manufacturers achieve the desired shape and intricacies of the final product. Moreover, small pins often serve as alignment mechanisms in die assemblies, ensuring precise alignment between die halves. By maintaining accurate alignment during the molding process, these pins contribute to the consistency and quality of the final molded parts.

Machining these pins can be achieved through turning, rolling, milling, and laser cutting [1]. Among these techniques, turning is particularly prevalent due to the widespread availability and affordability of machinery and the minimal requirement for skilled labor. In addition, machine productivity can be significantly improved when automation is implemented. The primary motion of turning is the rotation of the workpiece combined with the tool's translational motion to shape the surface. The cutting speed, v_c, is calculated using equation [2]:

$$v_c = \frac{\pi D_w n}{1000} \text{ (m/min)} \quad (1)$$

where D_w is the diameter of the workpiece (mm) and n is the rotational speed of the spindle (or workpiece) (rpm). In addition, other important parameters, such as feed rate (f), cut depth, as well as geometry and material of the cutting tool, also influence machining quality and productivity [3-6].

Ultrasonic vibration can assist the turning process in three ways: radial [7], feed rate [8], and cutting speed [9, 10]. The application of vibration aims to create specially structured surfaces [11] or reduce cutting force and tool wear [12, 13] for improved machined surface quality and performance. However, there are few studies that compare surface quality across different materials when employing ultrasonic vibration-assisted turning in the cutting speed direction for small shafts. For example, the authors in [14, 15] only provide the models to predict surface roughness when dry turning 6061-T6 Aluminum alloy and hard turning 080A67 steel. Therefore, the purpose of this work is to elucidate the impact of ultrasonic vibration on the turning process of C40 Carbon steel and 201 stainless steel. Farther, this study addresses the important parameters of assisted ultrasonic vibration, including frequency and vibration amplitude.

II. DESIGN THE HORN FOR ULTRASONIC ASISSTED TURNING

A. *Modal Analysis and Harmonic Response of the Horn*

Vibration for assisting in machining is generated by an alternating current generator operating at ultrasonic frequencies to apply a strong electric field to piezoelectric ceramic material. The material undergoes continuous compression and expansion in response to the fluctuating electric fields, generating mechanical vibrations. Assembled with front and back metal blocks and securely fastened by bolts, piezoelectric ceramic rings form ultrasonic piezoelectric transducers. The transducers produce mechanical waves with frequencies that match those of the electrical generator. However, the transmission of vibrations from the transducer to the turning tool requires the use of a horn. The horn, designed to resonate at the working frequency of the transducer and the ultrasonic generator, plays a crucial role in this process. Unlike rotary ultrasonic machining, ultrasonic welding, or ultrasonic cleaning, the design of the horn in ultrasonic assisted turning is often complex, making analytical calculations impractical. Modal analysis has therefore been employed for decades to determine the horn's natural frequency and harmonic response, which enables the prediction of vibration amplitudes at desired surfaces.

To begin, a preliminary estimate of the horn length is made, aiming for approximately half the wavelength using the formula [16]:

$$L_{Horn} = \frac{v}{2f} = \frac{1}{2f}\sqrt{\frac{E}{\rho}} \quad (2)$$

where v represents the sound speed in the horn (m/s), f is the vibration frequency (1/s), while E and ρ stand for the Young's modulus (Pa) and the density of the horn material (kg/m³), respectively. Therefore, selecting structural steel as the horn material (with E = 200 GPa and ρ = 7850 kg/m³) yields an estimated length of 126.2 mm. However, this calculation overlooks the presence of threaded holes, bolt, and turning insert. After performing the modal analysis for the entire system, the dimensions are adjusted accordingly, as depicted in Figure 1(a). Figure 1(b) illustrates the modal analysis image of the structure in Figure 1(a), featuring a turned insert CCMT09T304 made of Tungsten carbide (E = 634 GPa, ρ = 15.6 kg/dm^3). It showcases a natural frequency of 19991 Hz at the longitudinal vibration mode. Remarkably, according to simulation, substituting the CCMT09T304 turning insert with DNMG1504 results in a downward shift of the longitudinal mode's natural frequency to 19554 Hz as seen in Figure 2. Similarly, utilizing high-speed tool steel instead of Tungsten carbide for the CCMT09T304 insert yields a natural frequency of 20070 Hz. Moreover, according to (2), the horn length varies inversely with frequency for the same material, indicating that to operate at higher frequencies, the horn length must be shortened accordingly. Furthermore, the introduction of drilling holes in the center of the horn induces a comparable effect to shortening its length.

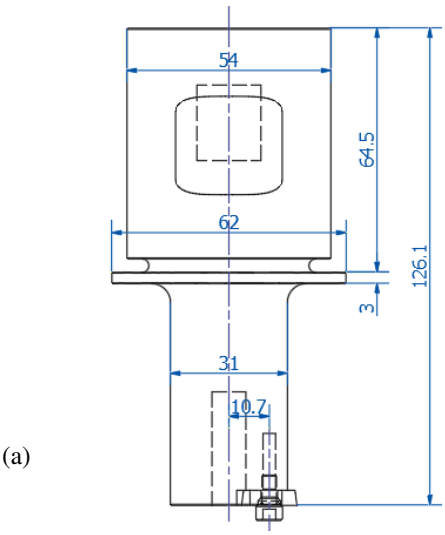

(a)

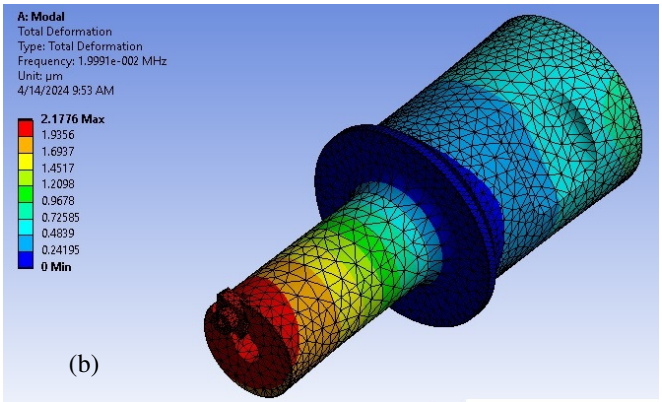

(b)

Fig. 1. (a) Drawing of the horn's structure, (b) Modal analysis of the horn with CCMT09T304.

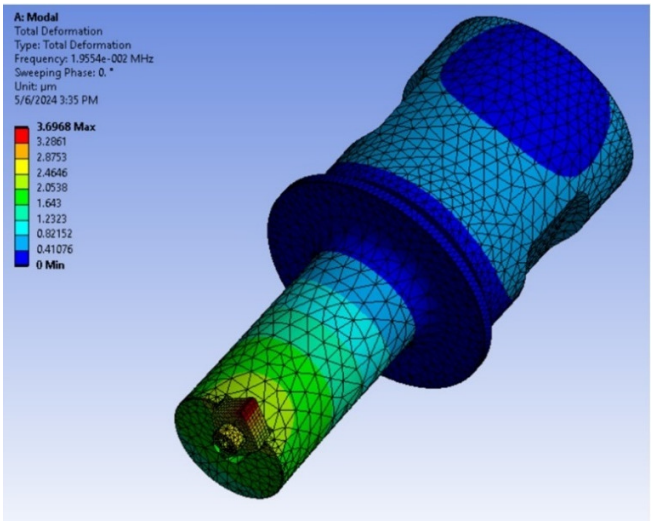

Fig. 2. Modal analysis of the horn with DNMG1504 turning insert.

B. Experiment Measurement of Vibration Amplitude of Turning Insert

The amplitude of the ultrasonic vibration depends on both the power of the ultrasonic generator and the amplification of the horn. Before initiating the Ultrasonic Assisted Turning (UAT) process, it is necessary to accurately determine the vibration amplitude to analyze the effects of UAT. The vibration frequency is determined by the generator and the natural frequency of both the transducer and horn systems, which remains relatively stable. However, during the turning process, the heat generated in the cutting zone induces changes in material properties, leading to a subsequent decrease in the working frequency. Measuring the vibration amplitude of the horn in real-time and amidst temperature fluctuations poses challenges. Therefore, simulation of the vibration amplitude was conducted in the frequency domain. Figure 3 illustrates the vibration amplitude around the resonant frequency of the horn. At a frequency of 19990 Hz, the simulation result indicates an amplitude of 14.9 µm when the input vibration amplitude at the end face of the 54 mm shaft is 6 µm. Verification of the vibration amplitude is carried out under laboratory conditions using the laser sensor LK-H055, with a working range of 50 ± 10 mm, repeatability of 0.025 µm, and a sampling frequency of 392/200/100/50/20/10/5/2/1 kHz.

Figure 4 shows the practical setup for measuring amplitude and the result of vibration amplitude measurements depicted as a graph of distances at various sampling locations. Utilizing a sampling frequency of 392 kHz (sampling cycle of 2.55 µs), which is approximately 20 times of the vibration period to be measured (around 50 µs), enables efficient data collection. The vertical distance from point A to point B is observed to be twice the amplitude, while the vibration period corresponds to the number of measuring points multiplied by 2.55 µs. The actual measurement of vibration amplitude was recorded at 16.3 µm, indicating a deviation of approximately 9.4% compared to the simulation. This difference is considered acceptable and is attributed to deviations in dimensions between the actual sample and the drawings, as well as variations in the material conditions and temperature.

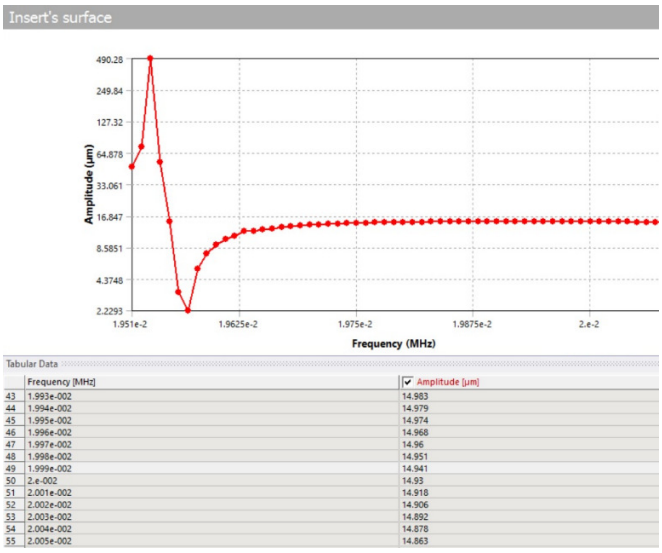

Fig. 3. Simulation of the amplitude of the vibration around the natural frequency of the horn.

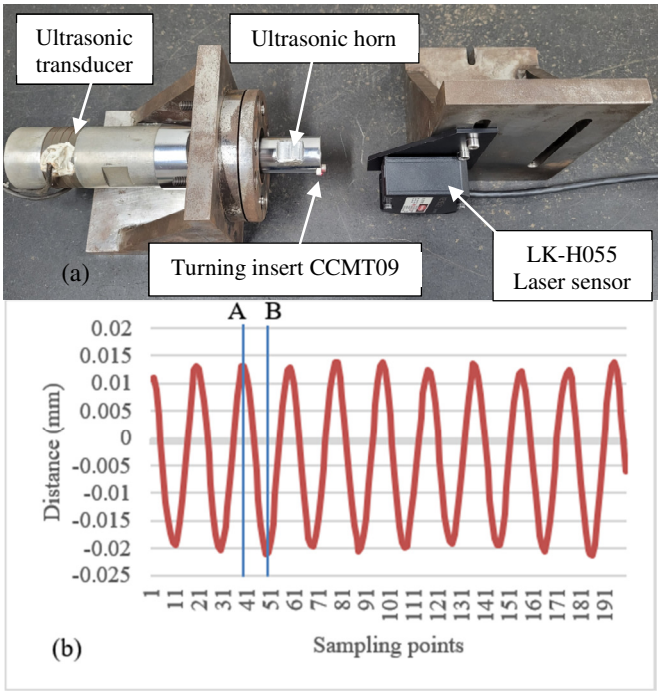

Fig. 4. (a) Practical setup for measuring amplitude, (b) Distance versus sampling points.

III. RESULTS AND DISCUSSION

The shafts, made of C40 steel and 201 stainless steel with a small diameter of around 9 mm, were machined on a traditional lathe, the OKK Ramo, with a maximum spindle speed of 2000 rpm. To compare the surface roughness between UAT and Conventional Turning (CT), the cutting parameters were maintained constant: a feed rate of 0.1 mm/rev and a cutting depth of 0.15 mm, while the cutting speed varied at 15, 24, and

36 m/min. Given the susceptibility of small shafts to mounting errors, which can induce vibrations, both UAT and CT processes were conducted under identical mounting conditions. Figure 5 depicts images of the shafts after turning at different cutting speeds. Subsequently, the roughness was measured using a Mitutoyo SJ301 roughness tester, as illustrated in Figure 6.

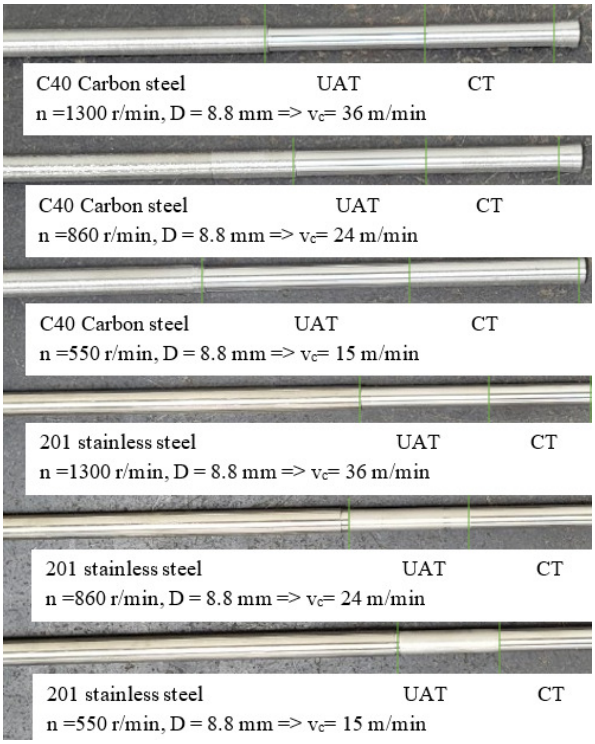

Fig. 5. The shafts were turned at ap = 0.15 mm, f = 0.1 mm/rev, and various cutting speeds.

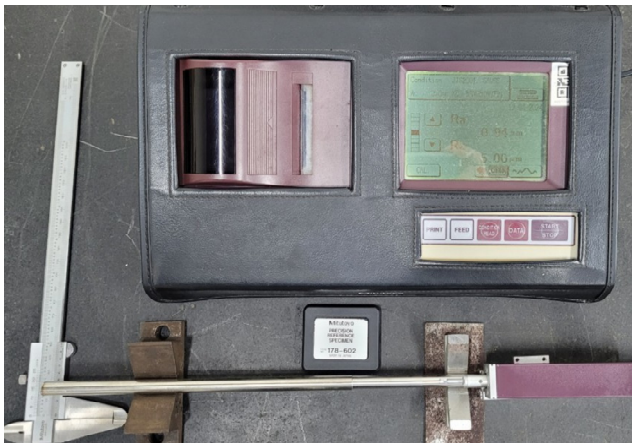

Fig. 6. The 201 stainless steel shaft was measured with the Mitutoyo surftest SJ301.

The charts in Figure 7 present the average results of three measurements at each cutting speed. The authors in [17] have reported surface roughness, Ra, values ranging from about 2.2 to 6 µm when dry turning AISI 1040 steel at a cutting speed of 135 m/min, over a machining time of up to 40 minutes. For 201 stainless steel, according to [18], the Ra ranges from 1.66 to 2.21 µm when the cutting speed is between 37 and 870 m/min. In addition, in [19], Ra ranging from 0.29 to 0.64 µm is reported for turning 420 stainless steel using the optimal SiO_2 nano-lubrication regime. These findings align with the surface roughness results obtained from CT in our work. However, slight differences were observed in the CT experiments for C40 steel, notably, the Ra improved by 63% as the cutting speed increased from 15 to 36 m/min. For stainless steel, with the same increase in cutting speed, Ra improved only by 22%.

This variance can be attributed to the significant influence of cutting heat on surface roughness. The 201 stainless steel, with a thermal conductivity of 16.2 W/mK, retains more heat compared to C40 Carbon steel, which has a thermal conductivity of 51.9 W/mK. As a result, during turning of stainless steel, the generated heat primarily transfers to the tool and chip, elevating temperatures in the cutting zone and promoting chip adhesion to the workpiece and tool. On the contrary, a substantial portion of cutting heat is absorbed by the C40 steel workpiece, which retards the rise of the temperature in the cutting zone and results in better surface roughness at higher cutting speeds [20]. The application of UAT to C40 steel demonstrates a significant improvement in roughness even at extremely low cutting speeds, but the same phenomenon is not clearly observed in stainless steel. Therefore, the effect of UAT on stainless steel is limited, since satisfactory roughness is achieved at low cutting speeds.

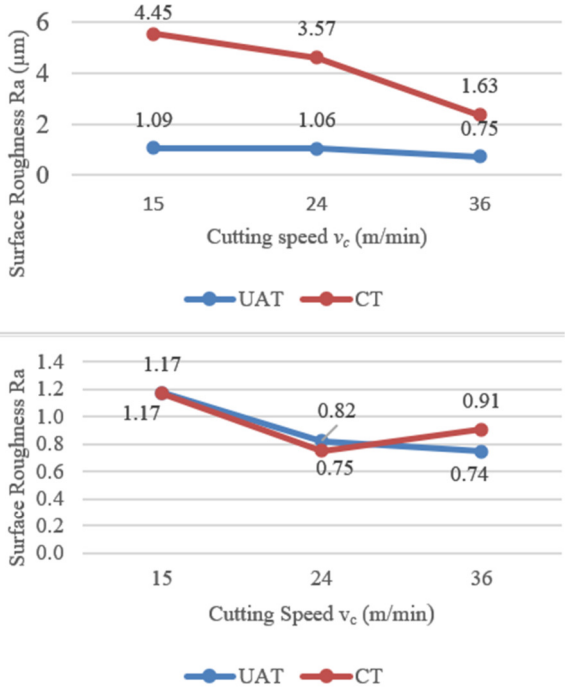

Fig. 7. Ra roughness parameter at various cutting speeds for: (a) C40 Carbon steel and (b) 201 stainless steel.

Figures 8 to15 display the roughness profiles of the surfaces machined by UAT and CT. Particularly, when machining with UAT at low spindle rotation speeds, the roughness profile

exhibits a widened shape at the bottom, whereas in CT, the profile assumes a triangular shape resembling that of the turning insert.

Fig. 8. Roughness profile of C40 Carbon steel with UAT at 550 rpm (*vc* = 15 m/min), *ap* = 0.15 mm, *f* = 0.1 mm/rev.

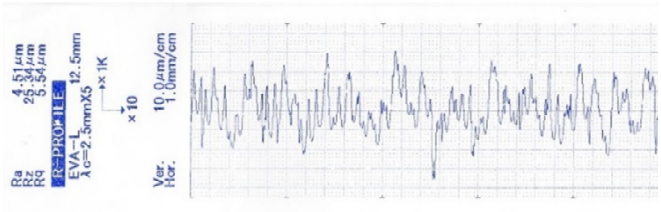

Fig. 9. Roughness profile of C40 Carbon steel with CT at 550 rpm (*vc* = 15 m/min), *ap* = 0.15 mm, *f* = 0.1 mm/rev.

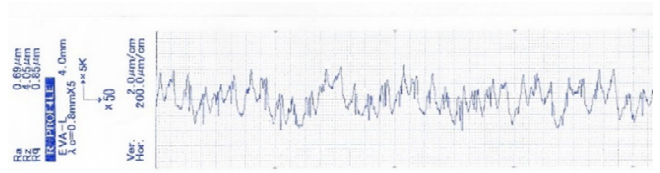

Fig. 10. Roughness profile of C40 Carbon steel with UAT at 1300 rpm (*vc* = 36 m/min), *ap* = 0.15 mm, *f* = 0.1 mm/rev.

Fig. 11. Roughness profile of C40 Carbon steel with CT at 1300 rpm (*vc* = 36 m/min), *ap* = 0.15 mm, *f* = 0.1 mm/rev.

Fig. 12. Roughness profile of 201 stainless steel with UAT at 550 rpm (*vc* = 15 m/min), *ap* = 0.15 mm, *f* = 0.1 mm/rev.

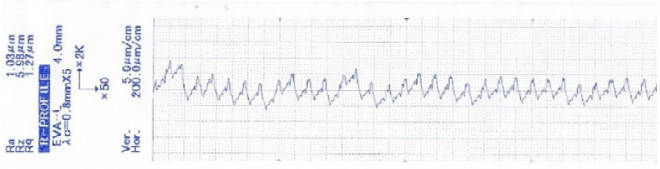

Fig. 13. Roughness profile of 201 stainless steel with CT at 550 rpm (*vc* = 15 m/min), *ap* = 0.15 mm, *f* = 0.1 mm/rev.

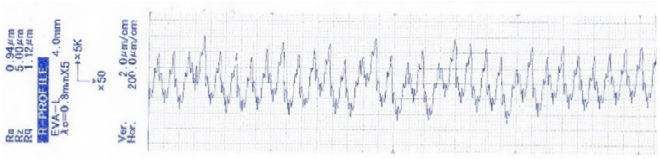

Fig. 14. Roughness profile of 201 stainless steel with UAT at 1300 rpm (*vc* = 36 m/min), *ap* = 0.15 mm, *f* = 0.1 mm/rev.

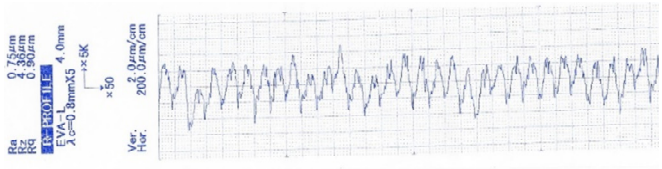

Fig. 15. Roughness profile of 201 stainless steel with CT at 1300 rpm (*vc* = 36 m/min), *ap* = 0.15 mm, *f* = 0.1 mm/rev.

IV. CONCLUSIONS

Based on the results of modal analysis, it becomes evident that the natural frequency of the horn changes greatly with its length and material. If the horn design in this study is changed, for example, changing the material of turning insert CCMT09T304 from Tungsten carbide to high-speed tool steel, the natural frequency of the whole system increases by 79 Hz (from 19991 to 20070 Hz), and using turning insert DNMG15 instead of CCMT09T304 results in a reduction of the natural frequency by 437 Hz (from 19991 to 19554 Hz). Controlling vibration amplitude also poses challenges because it depends greatly on the power generator and the horn's amplification factor. Measuring vibration amplitude at high frequencies can be used by laser displacement sensors, but requires a sampling frequency of at least 10 times the frequency to be measured for ensuring accurate measurement result.

Ultrasonic vibration has shown significant benefits in the turning process of small shafts, such as those at 9 mm in diameter, particularly evident in C40 Carbon steel. Here, the surface roughness Ra was reduced more than four times, from 4.45 to 1.09 µm, at a cutting speed of 15 m/min. With higher cutting speeds, its influence is clearly reduced because the additional cutting speed of ultrasonic vibration is not dominant compared to the traditional cutting speed. Conversely, the impact of ultrasonic vibration on 201 stainless steel is less pronounced, because low surface roughness can already be achieved at low cutting speeds.

ACKNOWLEDGMENTS

This research was funded by Hanoi University of Science and Technology, grant number T2022-PC-025.

REFERENCES

[1] A. Boudjemline, M. Boujelbene, and E. Bayraktar, "Surface Quality of Ti-6Al-4V Titanium Alloy Parts Machined by Laser Cutting," *Engineering, Technology & Applied Science Research*, vol. 10, no. 4, pp. 6062–6067, Aug. 2020, https://doi.org/10.48084/etasr.3719.

[2] V. P. Astakhov, "Turning," in *Modern Machining Technology*, 1st ed., Cambridge, UK: Woodhead Publishing, 2011, pp. 1–78.

[3] N. S. Kumar, A. Shetty, A. Shetty, A. K, and H. Shetty, "Effect of Spindle Speed and Feed Rate on Surface Roughness of Carbon Steels in

CNC Turning," *Procedia Engineering*, vol. 38, pp. 691–697, Jan. 2012, https://doi.org/10.1016/j.proeng.2012.06.087.

[4] İ. Asiltürk and H. Akkuş, "Determining the effect of cutting parameters on surface roughness in hard turning using the Taguchi method," *Measurement*, vol. 44, no. 9, pp. 1697–1704, Nov. 2011, https://doi.org/10.1016/j.measurement.2011.07.003.

[5] N. Qehaja, K. Jakupi, A. Bunjaku, M. Bruçi, and H. Osmani, "Effect of Machining Parameters and Machining Time on Surface Roughness in Dry Turning Process," *Procedia Engineering*, vol. 100, pp. 135–140, Jan. 2015, https://doi.org/10.1016/j.proeng.2015.01.351.

[6] A. Hasçalık and U. Çaydaş, "Optimization of turning parameters for surface roughness and tool life based on the Taguchi method," *The International Journal of Advanced Manufacturing Technology*, vol. 38, no. 9, pp. 896–903, Sep. 2008, https://doi.org/10.1007/s00170-007-1147-0.

[7] X. Liu, D. Wu, J. Zhang, X. Hu, and P. Cui, "Analysis of surface texturing in radial ultrasonic vibration-assisted turning," *Journal of Materials Processing Technology*, vol. 267, pp. 186–195, May 2019, https://doi.org/10.1016/j.jmatprotec.2018.12.021.

[8] Z. Xiangyu, L. Zhenghui, S. He, and Z. Deyuan, "Surface Quality and Residual Stress Study of High-speed Ultrasonic Vibration Turning Ti-6Al-4V Alloys," *Procedia CIRP*, vol. 71, pp. 79–82, Jan. 2018, https://doi.org/10.1016/j.procir.2018.05.075.

[9] G. S. Ghule *et al.*, "Investigation of conventional and ultrasonic vibration-assisted turning of hardened steel using a coated carbide tool," *Frontiers in Mechanical Engineering*, vol. 10, Apr. 2024, Art. no. 1391315, https://doi.org/10.3389/fmech.2024.1391315.

[10] R. Kang, P. Zhang, Z. Wei, Z. Dong, and Y. Wang, "Experimental Study on Ultrasonic Assisted Turning of GH4068 Superalloy," *Materials*, vol. 16, no. 9, Jan. 2023, Art. no. 3554, https://doi.org/10.3390/ma16093554.

[11] X. Liu, D. Wu, and J. Zhang, "Fabrication of micro-textured surface using feed-direction ultrasonic vibration-assisted turning," *The International Journal of Advanced Manufacturing Technology*, vol. 97, no. 9, pp. 3849–3857, Aug. 2018, https://doi.org/10.1007/s00170-018-2082-y.

[12] I. Llanos, Á. Campa, A. Iturbe, P. J. Arrazola, and O. Zelaieta, "Experimental Analysis of Cutting Force Reduction During Ultrasonic Assisted Turning of Ti6Al4V," *Procedia CIRP*, vol. 77, pp. 86–89, Jan. 2018, https://doi.org/10.1016/j.procir.2018.08.227.

[13] N. Khanna, J. Airao, C. K. Nirala, and G. M. Krolczyk, "Novel sustainable cryo-lubrication strategies for reducing tool wear during ultrasonic-assisted turning of Inconel 718," *Tribology International*, vol. 174, Oct. 2022, Art. no. 107728, https://doi.org/10.1016/j.triboint.2022.107728.

[14] M. H. El-Axir, M. M. Elkhabeery, and M. M. Okasha, "Modeling and Parameter Optimization for Surface Roughness and Residual Stress in Dry Turning Process," *Engineering, Technology & Applied Science Research*, vol. 7, no. 5, pp. 2047–2055, Oct. 2017, https://doi.org/10.48084/etasr.1560.

[15] B. T. Danh and N. V. Cuong, "Surface Roughness Modeling of Hard Turning 080A67 Steel," *Engineering, Technology & Applied Science Research*, vol. 13, no. 3, pp. 10659–10663, Jun. 2023, https://doi.org/10.48084/etasr.5790.

[16] A. S. Nanu, N. I. Marinescu, and D. Ghiculescu, "Study of ultrasonic stepped horn geometry design and FEM simulation," *Nonconventional Technologies Review*, vol. 4, pp. 25–30, 2011.

[17] N. R. Dhar, S. Paul, and A. B. Chattopadhyay, "The influence of cryogenic cooling on tool wear, dimensional accuracy and surface finish in turning AISI 1040 and E4340C steels," *Wear*, vol. 249, no. 10–11, pp. 932–942, Nov. 2001, https://doi.org/10.1016/S0043-1648(01)00825-0.

[18] A. I. Fernández-Abia, J. Barreiro, L. N. L. de Lacalle, and S. Martínez, "Effect of very high cutting speeds on shearing, cutting forces and roughness in dry turning of austenitic stainless steels," *The International Journal of Advanced Manufacturing Technology*, vol. 57, no. 1, pp. 61–71, Nov. 2011, https://doi.org/10.1007/s00170-011-3267-9.

[19] N. M. M. Reddy and P. K. Chaganti, "Investigating Optimum SiO2 Nanolubrication During Turning of AISI 420 SS," *Engineering, Technology & Applied Science Research*, vol. 9, no. 1, pp. 3822–3825, Feb. 2019, https://doi.org/10.48084/etasr.2537.

[20] H.-B. He *et al.*, "A study on major factors influencing dry cutting temperature of AISI 304 stainless steel," *International Journal of Precision Engineering and Manufacturing*, vol. 18, no. 10, pp. 1387–1392, Oct. 2017, https://doi.org/10.1007/s12541-017-0165-6.